

On the Saturation and Thermalization of Carbon Dioxide IV

by
Joseph Reynen
(updated April 18 2023)

PRINCIPIA
SCIENTIFIC



International

On the Saturation and Thermalization of Carbon Dioxide IV

Joseph Reynen

jwreynen@gmail.com

updated 18/04/2023

Introduction

This paper is an update of earlier papers [5].

Infra-red-active gases in the atmosphere are: water-vapor (H₂O), carbon dioxide (CO₂), methane (CH₄), ozone (O₃), laughing gas (N₂O)...

They hinder long-wave (LW) radiation to outer space from the surface of the planet to evacuate the heat which the sun is sending to the planet as short-wave (SW) radiation.

The most important infra-red-active gases are H₂O vapor and CO₂ gas.

In earlier papers the author has studied the hindering of the LW evacuation of heat from the terrestrial surface to outer-space by a mechanism of a stack of fine gauze, simulating the infra-red-active gases.

The paper mentions the International Panel on Climate Change (IPCC), which gives alarming messages to the general public by ignoring the physical phenomena thermalization and saturation of CO₂ with the excuse of their slogan: "*science is settled*".

Stack model to study the evacuation of heat from the planet.

A finite element method (FEM) has been used.

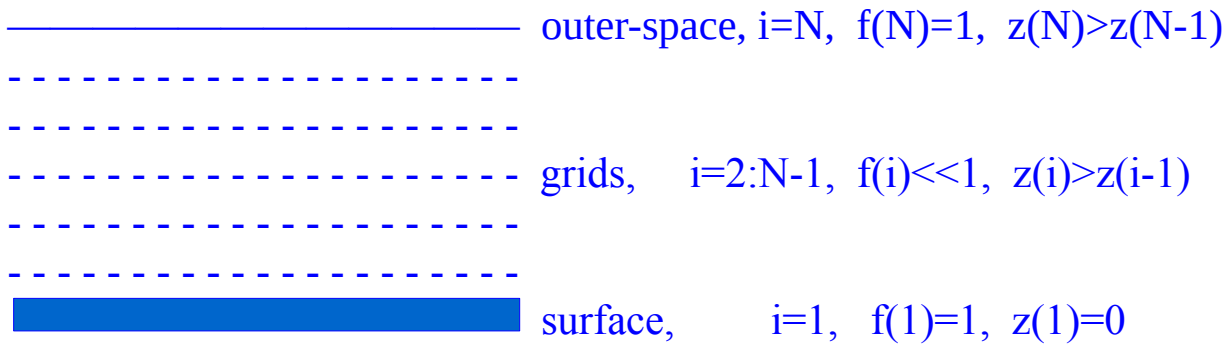
Not in the classical way of solving differential equations, but rather using FEM strategies to model the phenomenon and to deal with a great number of simultaneous algebraic relations using matrix notations [1].

We give a short description of the FEM approach.

We consider in **figure 1** a stack of $N-2$ grids, with dimensionless very small absorption coefficients $f(i) \ll 1$, being the ratio of the cross-section of the wires divided by the total surface. The absorption coefficients are assembled in a vector denoted by a bold character \mathbf{f} of order N , including $f(1)=1$ for the surface and $f(N)=1$ for outer-space.

We define $f_{tot} = \text{sum}(\mathbf{f}) - 2$, being the sum for the atmospheric grids.

Figure 1 Stack of fine gauze



Consider two layers of black grids with coefficients $f(i)$ and $f(j)$, and absolute temperatures [Kelvin], $T(i)$ and $T(j)$ respectively. According to the classical Stefan-Boltzmann relation with $\sigma = 5.67e-8$, the heat flux ϕ by LW radiation between the two grids can be written as :

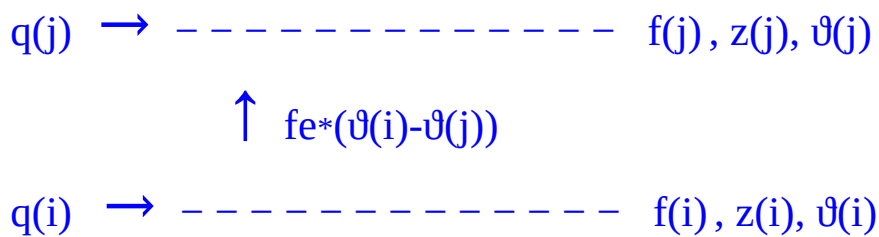
$$\phi(i \rightarrow j) = f(i)*f(j)*\sigma*(T(i)^4 - T(j)^4) \text{ and } \phi(j \rightarrow i) = 0 \text{ for } T(i)>T(j) \quad (1)$$

With $\vartheta = \sigma * T^4$ and $fe = f(i)*f(j)$ relation (1) can be written as:

$$\phi(i \rightarrow j) = fe*(\vartheta(i)-\vartheta(j)) \quad \text{and} \quad \phi(j \rightarrow i) = 0 \quad \text{for } \vartheta(i)>\vartheta(j) \quad (1a)$$

This is the one-stream energy formulation without the nonphysical back-radiation of the two-stream Schwarzschild formulation of 1906. A radiation finite element with nodal parameters is depicted in **figure 2**.

Figure 2 Radiation finite element



- Nodal parameters:
- f absorption coefficient
 - z coordinate [m]
 - ϑ variable representing $\sigma*T^4$ [W/m²]
 - q external heat load into the grids [W/m²]

Constitutive relation : fe element radiation coefficient

By means of a Galerkin-type of variation process, the element heat balance can be written as:

$$\begin{vmatrix} q(i) \\ q(j) \end{vmatrix} = \begin{vmatrix} fe & -fe \\ -fe & fe \end{vmatrix} \begin{vmatrix} \vartheta(i) \\ \vartheta(j) \end{vmatrix} \quad (2)$$

Equations (2) describe, for given $\vartheta(i)$, $\vartheta(j)$ and fe , the flow of heat by LW radiation between grids i and j and the necessary external heat sources $q(i)$ and $q(j)$, for a balance.

For an element with grids in **adjacent** levels i and $j = i+1$, the element transfer coefficient is indeed $fe = f(i)*f(j)$.

However, elements of the type of **figure 2** can be overlapped with each other. When between grid i and grid j of one element other grids of other elements are present, the transfer of heat by radiation between grid i and grid j will be hindered and fe of element (i, j) with $j>i+1$ becomes :

$$fe = f(i)*\text{viewfactor}(i, j)*f(j) \quad (2a)$$

In (2a) the $\text{viewfactor}(i, j)$ takes into account the fact that other grids k are present between grid i and grid j of an element (i, j) .

The $\text{viewfactor}(i, j)$ between the nodes i and j can be written as:

$$\text{viewfactor}(i, j) = 1 - \sum f(k) \quad \text{for} \quad z(i) < z(k) < z(j) \quad (2b)$$

The element matrices for the different pairs of grids are assembled in a symmetric system matrix, denominated by a bold character **K**.

For a stack with N levels there are $N(N-1)/2$ pairs with a balance like (2) and the system matrix **K** is of order $N \times N$. We use N up to 90 nodes.

Nodal parameters $\vartheta(i)$ and nodal heat loads $q(i)$ are assembled in vectors of order N , denominated with bold characters **ϑ** and **q** , respectively.

The characteristic equations of the atmospheric LW radiation become :

$$q = K*\vartheta \quad (3)$$

The vector relation (3) represents N algebraic relations: for given values of the components of the vector **ϑ** and of the matrix **K** one obtains the vector **q** of external thermal loads into the stack with $\text{sum}(q) = 0$, for a balance.

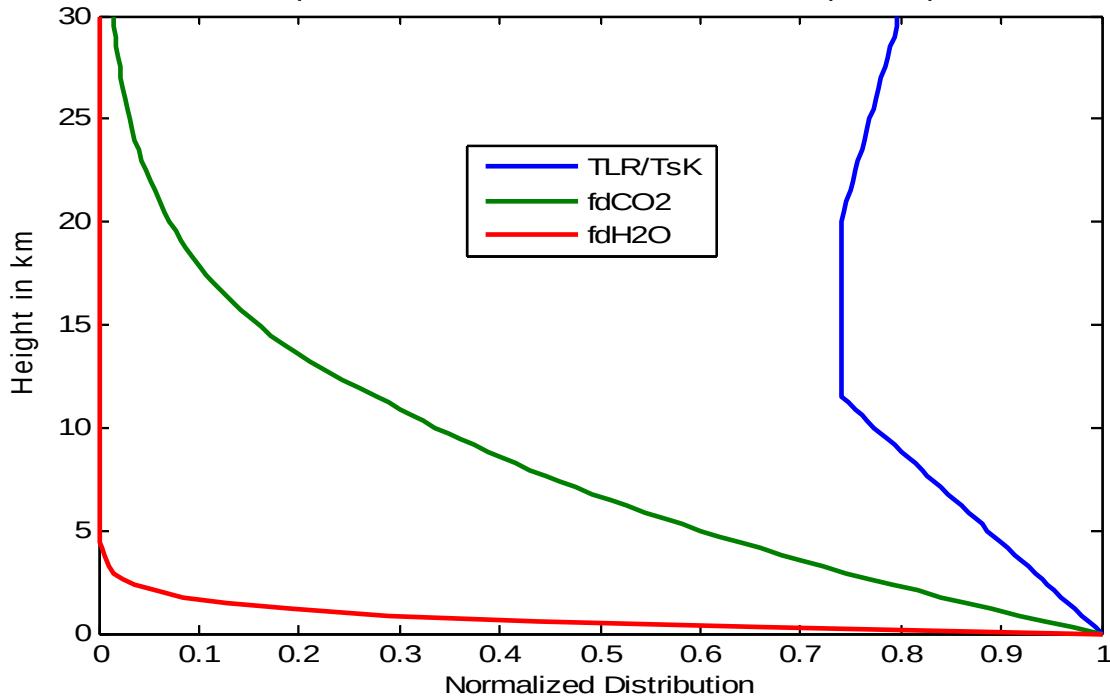
Data for the components of the vector ϑ and the matrix K

Data for these components are shown in **figure 3**: temperature distribution and concentration of water vapor H_2O and of carbon dioxide gas CO_2 over a height of 30 km.

NB *In computer language subscripts are not used. From now on, in this paper, we do not write anymore H_2O , CO_2 but $H2O$, $CO2$.*

Figure 3

fig 4.3 Normalized Temperature for $TsK=288$, water vapor for $m = 7$ and CO_2 distribution Lower atmosphere $ELR= -6.5$ K/km. Standard atmosphere up to 30 km



For a height up to 11.5 km the temperature is defined by the surface temperature and the environmental lapse rate, $ELR = -6.5$ °C/km.

It is the basis of the analysis of the heat evacuation through an atmosphere with only water-vapor.

The temperature distribution is converted to the variables $\vartheta(i)$ assembled in the vector ϑ . With the surface temperature TsK we get $TLR(i)$ and $\vartheta(i)$:

$$TLR(i)=TsK + ELR*z(i) \quad \text{and} \quad \vartheta(i) = \sigma*(TsK +ELR*z(i))^4 \quad (4)$$

Where $z(i) < 11.5$ is the vertical coordinate of the grid in km.

For $z(i) > 11.5$ km – for the CO_2 analyses – the temperature distribution follows from **figure 3**, which corresponds to the standard atmosphere.

Outer-space temperature is zero $K = 0$ or $\vartheta(N) = 0$.

In **figure 3** are also depicted the normalized distribution of H₂O vapor and of CO₂ gas: fd_{H_2O} and fd_{CO_2} , respectively.

The normalized H₂O distribution is defined heuristically by an exponential drop :

$$fd_{H_2O}(z) = \exp(-m \cdot z / \text{height}_5)$$

The coefficient $m = 7$, for a reference height_5 of 5 km, is obtained by comparing the results with the mainstream papers on the subject.

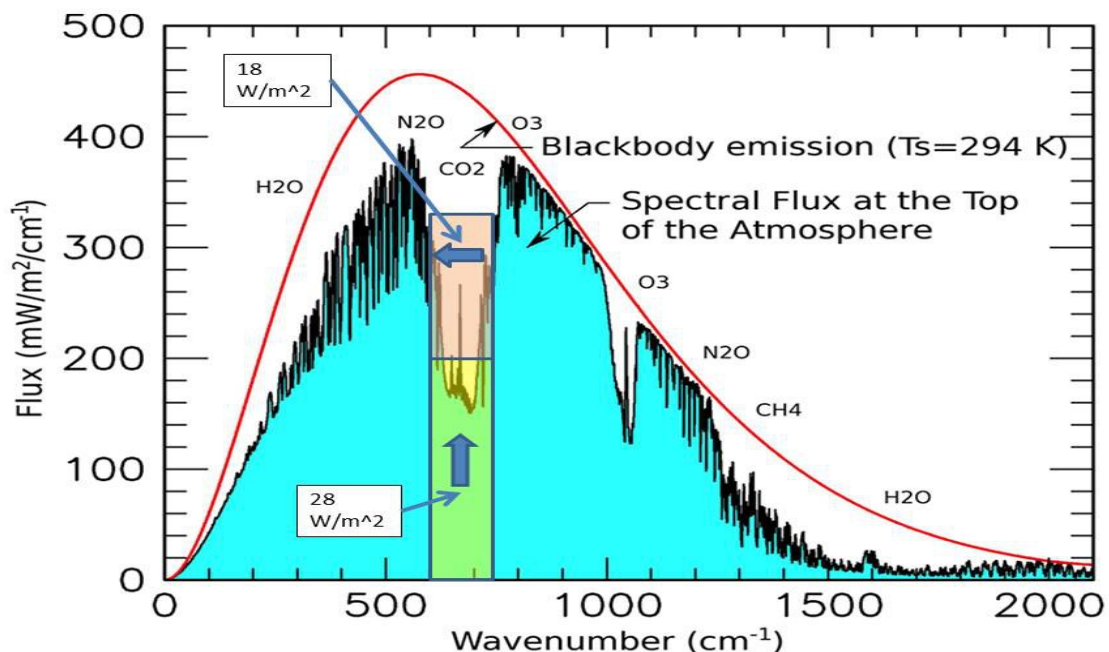
The CO₂ distribution is taken proportional to the height dependent air density in the atmosphere, assuming the volumetric concentration of CO₂ is constant over the height. More details are given in [1].

Fractions of H₂O and CO₂ in the LW terrestrial spectrum

From **figure 4** we can conclude that the fraction of CO₂ in the spectrum is $28 + 18 = 46 \text{ W/m}^2$ of the total Prevost flux $= \sigma \cdot T_s K^4 = 394 \text{ W/m}^2$ for a surface temperature of $T_s K = 288.72$:

$$\text{fraction}_{CO_2} = 0.1168 \quad \text{and} \quad \text{fraction}_{H_2O} = 1 - \text{fraction}_{CO_2} = 0.8832$$

Figure 4 from Pangburn blog [2]



Thermal radiation from below assessed from top-of-atmosphere.

Original graph from NASA

NB $T_s = 294 \text{ K}$ in **figure 4** is a reference value for the red Planck curve.

Other data are for a temperature of $T_s K = 288.72$ [K].

Results of stack model for water-vapor.

From **figure 3** we see, for the evacuation of heat through an atmosphere with only water-vapor, a model with a height of 11.5 km is sufficient. The computer program includes a mesh generator with element sizes based on geometric series: for N=40 nodes of order of 2 meter at the surface and of 2 km at 11.5 km height.

Figure 5 gives a graphical display of the vector relation (3): $\mathbf{q} = \mathbf{K} * \mathbf{\theta}$.

It might be useful to repeat in words what the vector relation means: *for a measured temperature distribution given in 40 nodes by a vector of parameters $\mathbf{\theta}$ of order 40 and by multiplication by a radiation matrix \mathbf{K} for water-vapor of order 40x40, one obtains a vector \mathbf{q} of order 40.*

What is the physical interpretation of the components of the vector \mathbf{q} ?

They represent: $q(1) = q_{surf} =$ LW surface flux of water-vapor

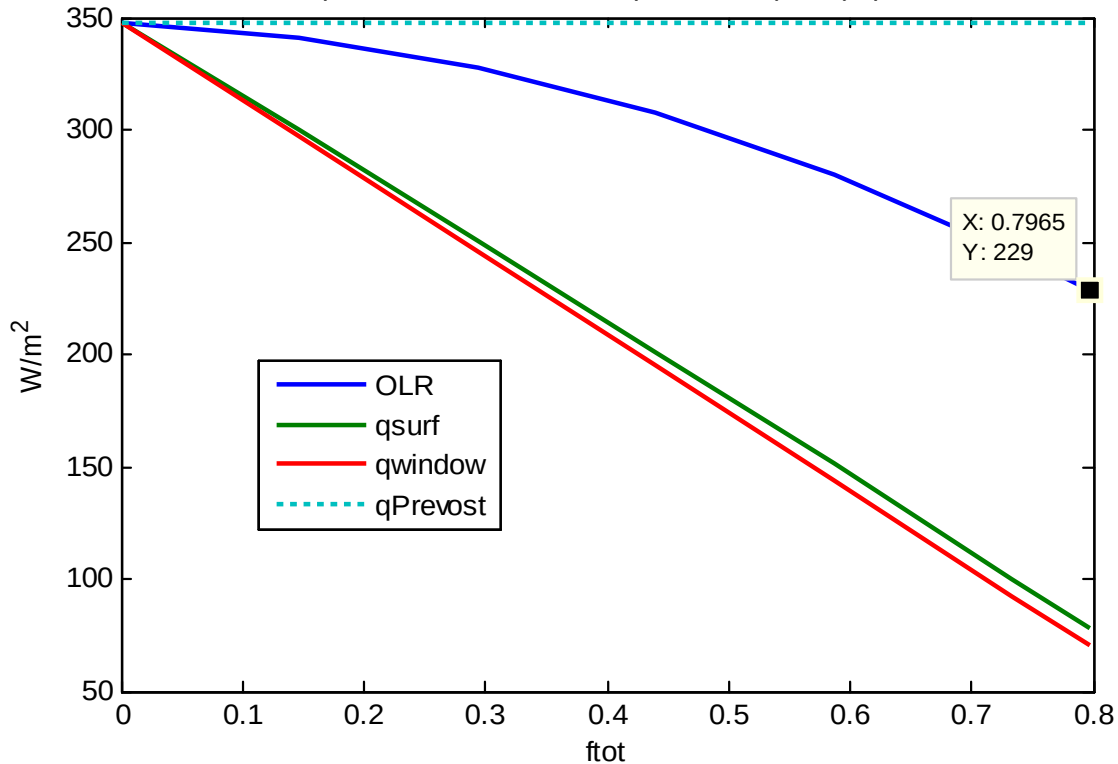
$-q(N) = OLR =$ outgoing LW radiation of water-vapor

We see in **figure 5** these two components of the vector \mathbf{q} , as well as

$$q_{Prevost} = fractionH2O * \sigma * TsK^4 = fractionH2O * \theta(1).$$

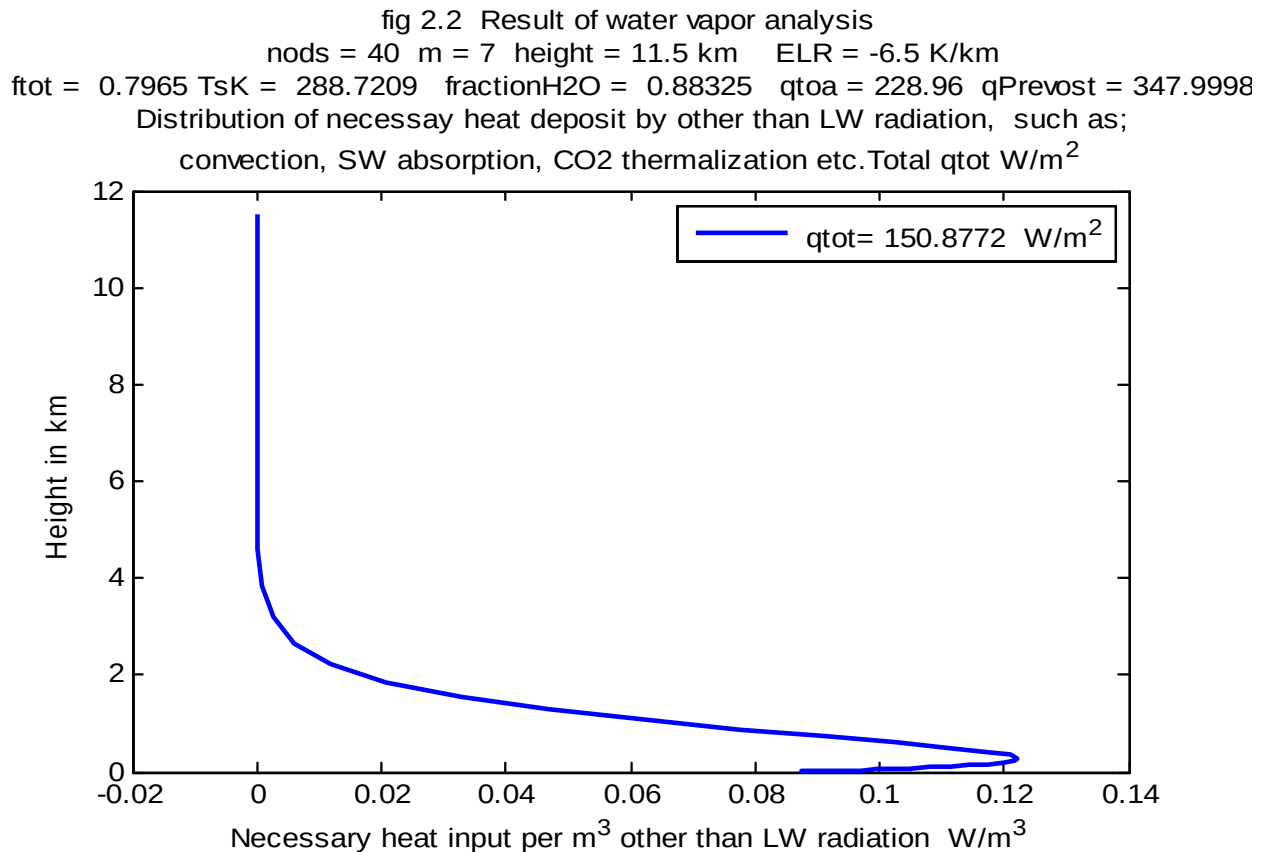
Figure 5

fig 2.1 Result of water vapor analysis
 nods = 40 m = 7 height = 11.5 km ELR = -6.5 K/km
 ftot = 0.7965 TsK = 288.7209 fractionH2O = 0.88325 qtoa = 228.96 qPrevost = 347.9998
 OLR, qsurf as function of ftot. qwindow = (1-ftot)*qPrevost



OLR_{H2O} of 228.96 W/m² is the average of the global outgoing LW radiation at H2O frequencies, for which the stack model gives ftot= 0.7965 and a window of (1-ftot) = 0.2035. With OLR_{CO2} = 11.04 from **figure 8**, the average total outgoing flux at top of atmosphere is: qtoa = 240 W/m². The calculated values of the other components of **q** are given in **figure 6**, not as nodal values with dimension W/m² but as distribution in W/m³.

Figure 6



These additional sources of heat are needed, in order that the temperature distribution indeed corresponds to the measured one, shown in **figure 3**. The stack model calculates, apart from LW radiation, the necessary additional heat input distribution with a total value of: 150.8772 W/m². Possible other heat inputs are from:

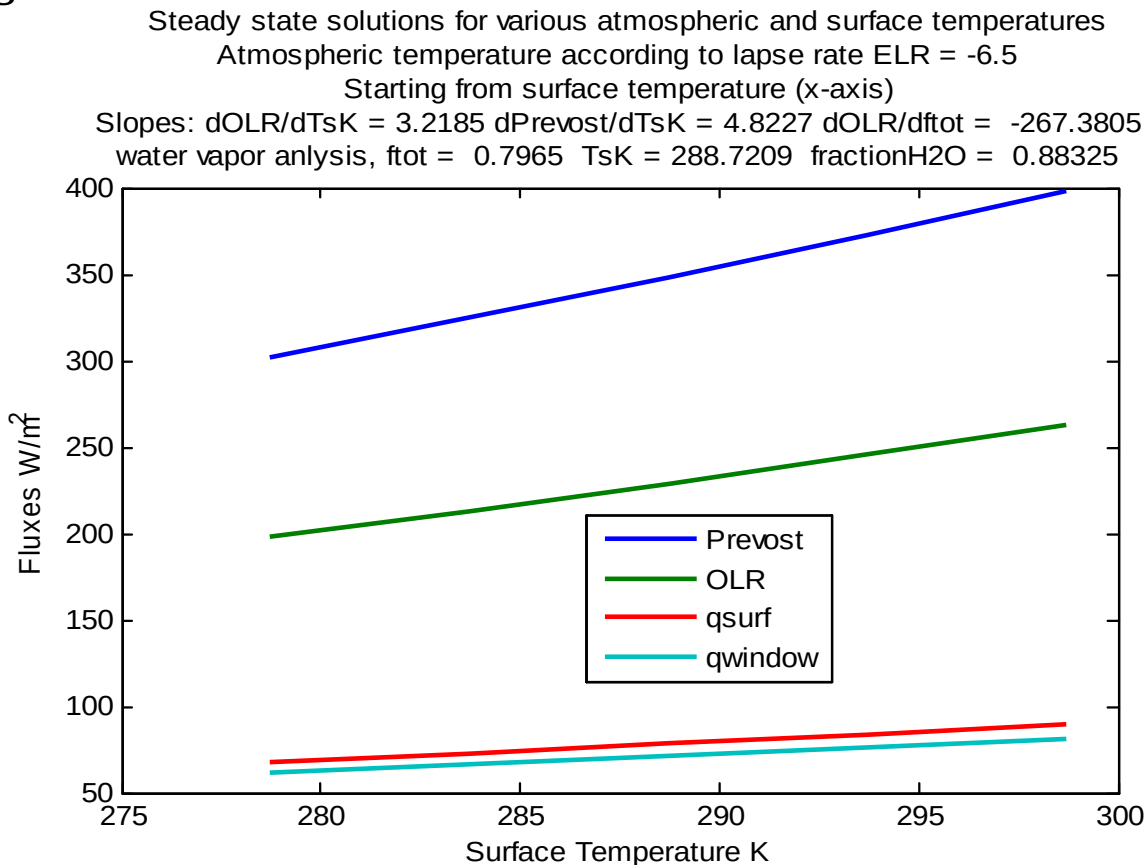
- *absorption of incoming SW radiation by aerosols*
- *convection from the surface of sensible and latent heat, and*
- *thermalization of CO2 i.e. absorbance in the atmosphere of a part of the infra-red-active gas by LW radiation from the surface but not re-emitted. The heat is given by collisions to the bulk of the atmospheric molecules: 79 % N2, 20 % O2 and the trace gas water-vapor H2O.*

These additional sources of heat are needed, in order that the temperature distribution indeed corresponds to the measured one, shown in **figure 3**. The first two contributions are also mentioned by mainstream authors on the subject, the third possible contribution, the thermalization of CO2 introduced in AD 2016 by Pangburn [2], is ignored by IPCC: remember their slogan "*science is settled*". We come back on thermalization later.

Dependence of OLR on surface temperature

For studies related to the dependence on the ambient temperature of the evacuation of heat from the planet by LW radiation, we need the variation of OLR with the surface temperature T_{sK} .

Figure 6a



We see from the slopes $dOLR/dT_{sK} = 3.2185 \text{ W/m}^2/\text{ }^\circ\text{C}$

We find a relation for the increase of OLR due to the surface temperature increase. We use the IPCC name for it, forcingOLR:

$$\text{forcingOLR} = (dOLR/dT_{sK}) * \Delta T_{sK} \quad [\text{W/m}^2] \quad (5)$$

Saturation of infra-red-active gas layers

In **figure 7** are given the results of analyses for water-vapor concentrations with $ftot > 1$.

We see that the OLR is not decreasing any more for $ftot > 1$.

The phenomenon is called saturation and is explained by equation (2b), repeated here:

$$\text{viewfactor}(i, j) = 1 - \sum f(k) \quad \text{for} \quad z(i) < z(k) < z(j) \quad (2b)$$

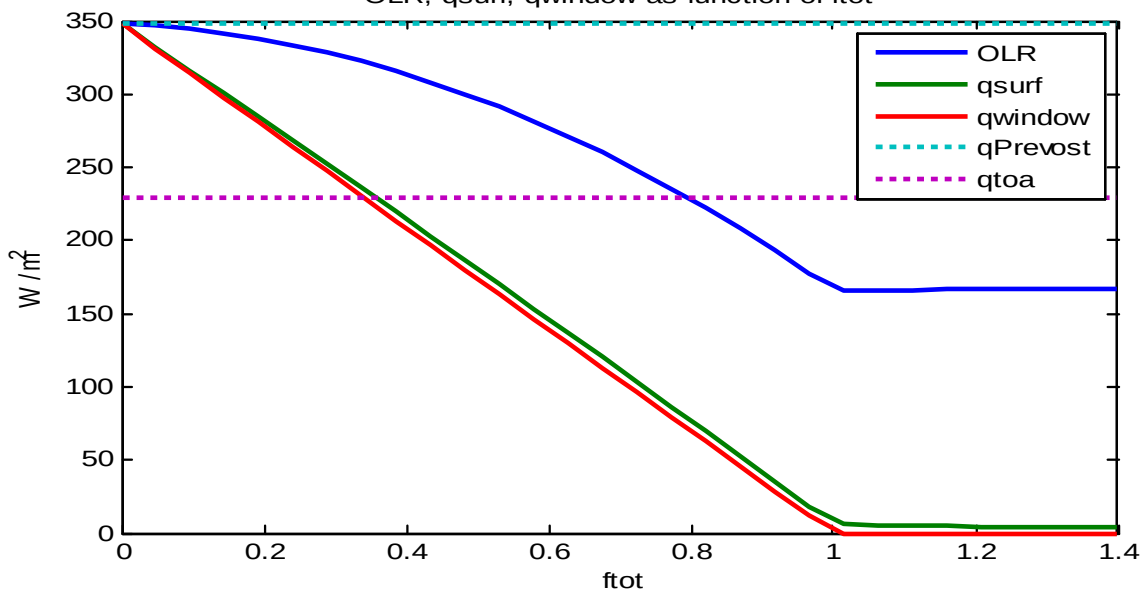
For $\sum f(k) > 1$, $\text{viewfactor}(i, j)$ becomes negative and it is put to zero.

For $\text{viewfactor}(i, j) = 0$ there is no LW heat transfer between nodes i and j .

The viewfactor can be regarded as a "window", we have not used that name because window is already used for other optical properties.

Figure 7

fig 3.1 The "saturation" phenomenon for water vapor by the stack model
 nods = 40 m = 7 height = 11.5 km ELR = -6.5 K/km
 $ftot = 1.4$ $TsK = 288.7209$ $\text{fractionH2O} = 0.88325$ $qtoa = 228.96$ $qPrevost = 347.9998$
 OLR, $qsurf$, $qwindow$ as function of $ftot$



The saturation phenomenon does not appear for water-vapor layers with $ftot < 1$. It is shown here for a water-vapor layer, for demonstration purposes only, because it is important for CO2 analyses further on, with $ftotCO2 > 1$.

IPCC is ignoring the CO2 saturation phenomenon, although it is one of the two reasons — *saturation and thermalization of CO2* — for the planet not heating up, as will be shown in the next sections.

Results of the stack model for CO2

The stack model for H2O is a one-stream, mono-chromatic model of the evacuation of heat from a planet with only water-vapor. It turns out to be accurate enough when compared to the results of mainstream authors on the subject, adjusted for the non-physical back-radiation in the two stream models. It can also be used for the analysis of CO2 with saturation for values of $f_{\text{totCO2}} > 1$.

For the CO2 analysis we take a model with a height of 30 km with the three 3 temperature zones, according to **figure 3**.

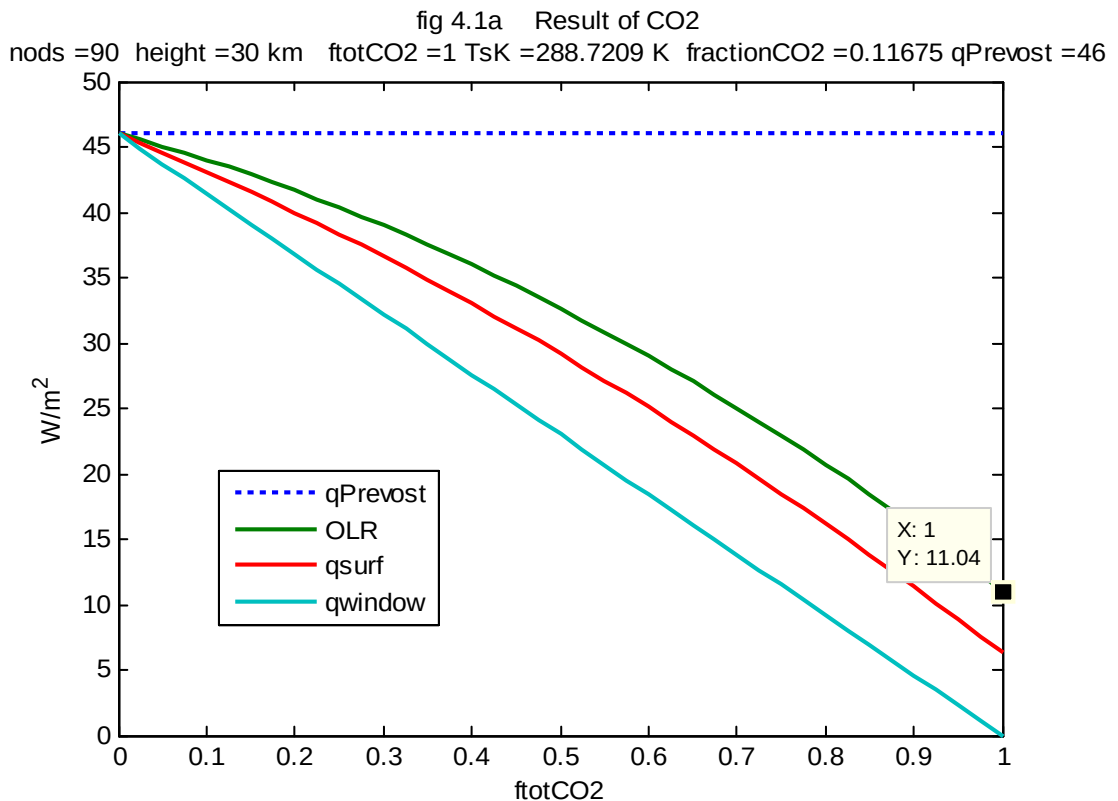
We use $N = 90$ nodes to model the three zones: 60, 15 and 15.

The results of the vector relation **(3)** for CO2, $\mathbf{q} = \mathbf{K} \cdot \boldsymbol{\vartheta}$, are given in **figure 8**, which is equivalent to **figure 5** for the water vapor analysis.

The components of \mathbf{q} and q_{Prevost} represent now:

$$\begin{aligned} q(1) &= q_{\text{surf}} = \text{LW CO2 surface flux} \\ -q(N) &= \text{OLR} = \text{outgoing LW CO2 radiation} \\ q_{\text{Prevost}} &= \text{fractionCO2} \cdot \sigma \cdot T_{\text{sK}}^4 = \text{fractionCO2} \cdot \vartheta(1). \end{aligned}$$

Figure 8 *no thermalization and no saturation*



Surface temperature increase due to CO2

In **figure 8** we see a decreasing OLR_{CO_2} flux, from $q_{Prevost} = 46 \text{ W/m}^2$ for $ftotCO_2 = 0$ towards lower values. The decrease ΔOLR_{CO_2} as function of OLR_{CO_2} becomes:

$$\Delta OLR_{CO_2} = - (q_{Prevost} - OLR_{CO_2}) \quad (6)$$

In order to keep the total OLR constant, the necessary increase of OLR_{H_2O} due to the increase of the surface temperature TsK , is the opposite:

$$\text{forcingOLR} = - \Delta OLR_{CO_2} = (q_{Prevost} - OLR_{CO_2}) \quad (6a)$$

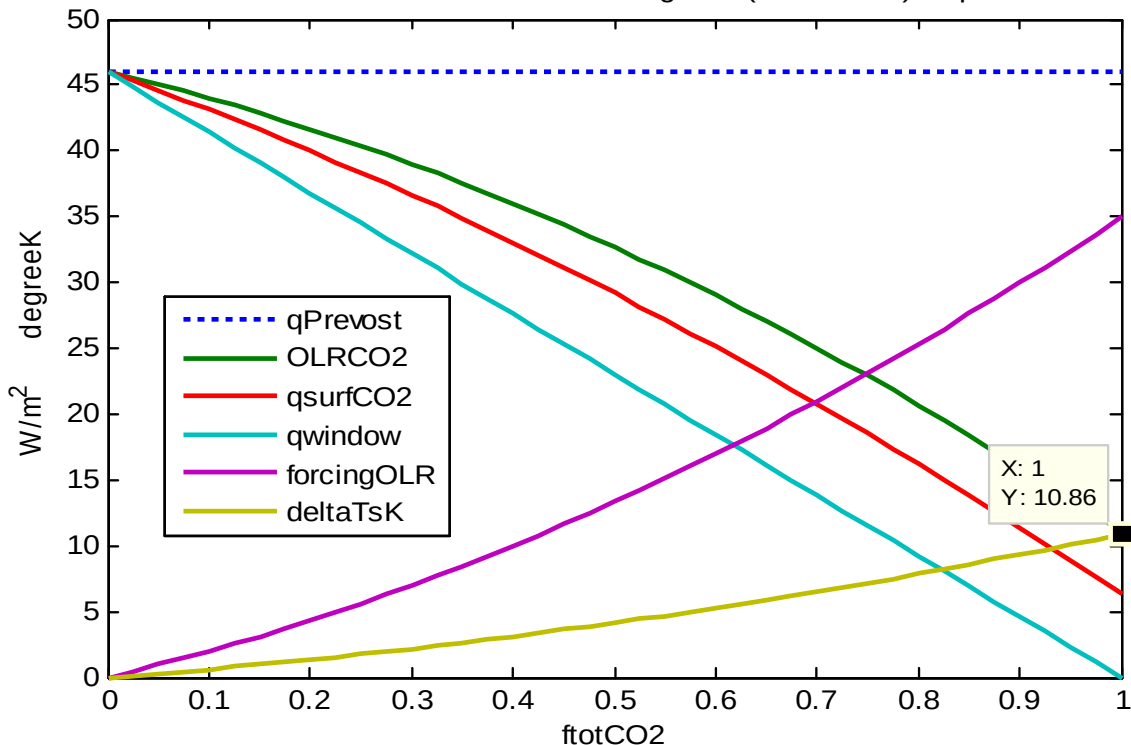
With the corresponding temperature increase from equation (5) repeated here:

$$\Delta TsK = \text{forcingOLR} / (dOLR/dTsK) \quad (5)$$

In **figure 8a** are given the results from equations (5) and (6a) for CO2 concentrations from $ftotCO_2 = 0$ to 1, or 400 ppm.

Figure 8a *no thermalization and no saturation*

fig 4.1a Result of CO2
 nods =90 height =30 km $ftotCO_2 = 1$ $TsK = 288.7209 \text{ K}$ $\text{fractionCO}_2 = 0.11675$ $q_{Prevost} = 46$
 $dOLR/dTsK = 3.2185$ $\Delta TsK = \text{forcingOLR} / (dOLR/dTsK)$ $q_{therm} = 0$



Historical omissions by IPCC authors

In this paper the stack model is used to analyze the hindering of LW radiation by infra-red-active gases like water vapor H₂O and carbon dioxide CO₂, respectively in **figures 5 and 8**.

With the two-stream Schwarzschild procedure of AD 1906 one can obtain similar results but they are seldom shown in detail by IPCC authors, for values of $f_{\text{totCO}_2} = 0$ to 1.

It is an advantage of the stack model with efficient graphical display that results can be shown, and not only for one single CO₂ concentration. The slope of the ΔT_{SK} curve in **figure 8a** at the point $f_{\text{totCO}_2} = 1$ becomes 16.38 °C and the average slope from $f_{\text{totCO}_2} = 0$ to 1 is 10.86 °C. The so-called sensitivity analysis for double CO₂ concentration, for the theory behind **figure 8a**, could be represented by these slopes.

It were this kind of temperature increases that James Hansen was referring to, in the congressional hearing of 23 June 1988, organized by then senator Al Gore.

It was difficult to look into the future by extrapolation.

However the temperature of the pre-industrial period of 280 ppm was known by measurement and much smaller than the value of 6.52 °C from **figure 8a** for $f_{\text{totCO}_2} = 0.7$.

From the very beginning skeptics have argued that when the theory underlying **figure 8a** is not accurate to explain the past, one cannot claim for the extrapolation towards higher CO₂ concentrations: obviously: "*science is settled*" is wrong.

Nevertheless, the value $\Delta T_{\text{SK}} = 10.86$ °C for $f_{\text{totCO}_2} = 1$ remained to be the temperature from the Schwarzschild analyses, still in use by alarmists and even by some skeptics as starting point for future temperature analyses.

Already in AD 2016, Pangburn [2] has given the reason for the high numbers in **figure 8a**: thermalization of CO₂.

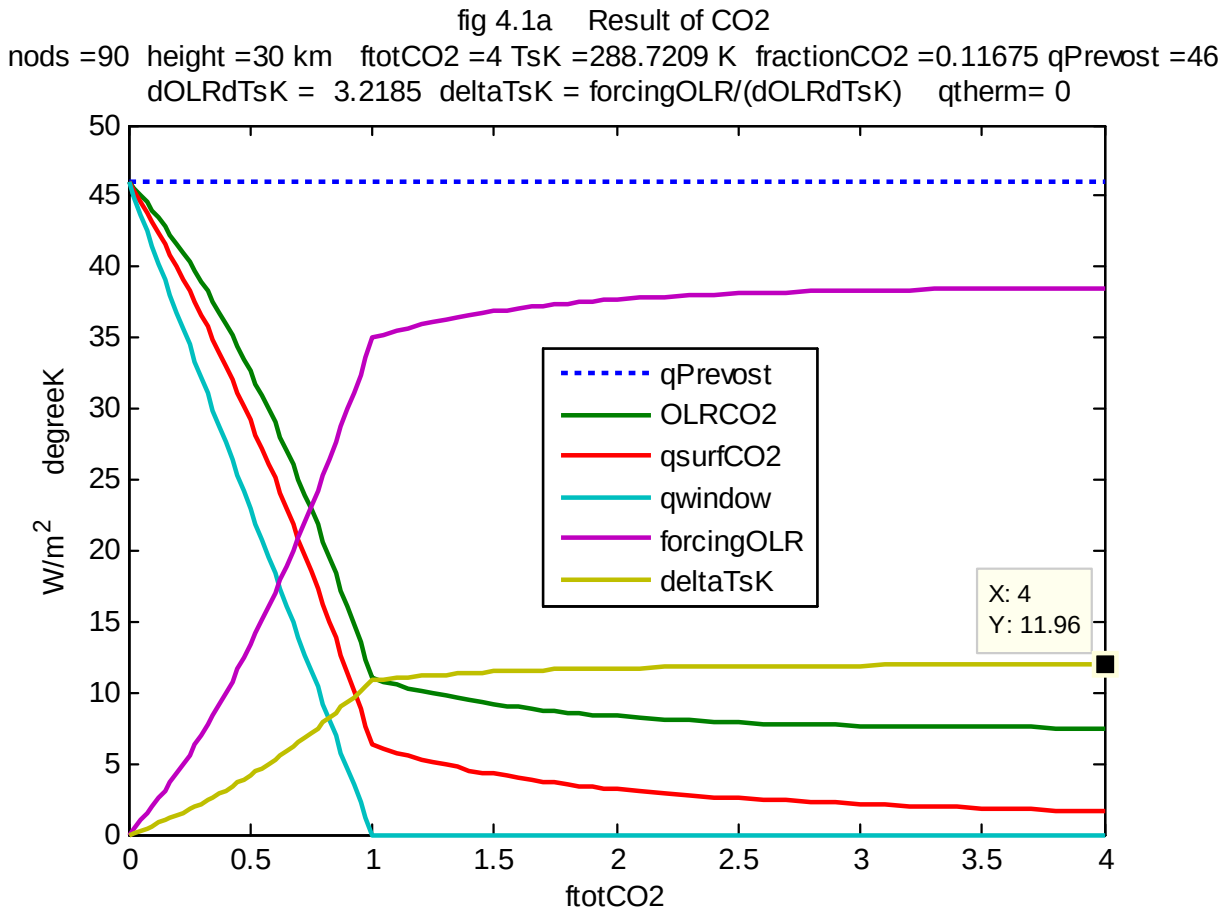
We come back to the thermalization phenomenon further on.

Saturation of carbon dioxide.

Saturation of CO₂ is another phenomenon ignored by IPCC with the excuse of their slogan: "*science is settled*".

Saturation results for CO₂ concentrations beyond 400 ppm are shown in **figure 8b**, up to $ftotCO_2 = 4$, or 1600 ppm.

Figure 8b *with saturation only, no thermalization*



The temperature increase from $ftotCO_2 = 1$ up to $ftotCO_2 = 4$ is small:
 $11.96 - 10.86 = 1.1$ °C

These small temperature increases beyond $ftotCO_2 = 1$, agree with the Happer numbers as shown in version II of this paper [5].

We note that for $ftotCO_2 = 1$ the $deltaTsK$ value around 10.86 °C is too high because thermalization has not been taken into account.

Happer insisted indeed to have only analyzed the temperature increase between $ftotCO_2$ values 1 and 2.

Thermalization of carbon dioxide

The classical Stefan-Boltzmann relation **(1)** assumes that the information exchange concerning the temperatures between surfaces and thereby exchange of energy is immediate.

There are however different time delays in the process, according to Pangburn **[2]**.

Relaxation time:

The time it takes for absorbed energy to be shared with surrounding molecules. It is of the order of a few microseconds.

Decay time:

The time between the absorption process of a molecule CO₂ and the re-emission process, it averages about 1.1 second.

Since the relaxation time is much smaller than the decay time, a CO₂ molecule in the absorption phase collides many times with surrounding 79% nitrogen N₂ molecules and 20% oxygen O₂ molecules, as well as with infra-red-active H₂O vapor molecules.

The CO₂ molecule loses the surplus energy before it has been built up completely for re-emission.

The CO₂ molecule is said to be thermalized, the surplus energy goes to the bulk of the molecules of the atmosphere. The exchanged energy has lost its CO₂ identity, the broad band of H₂O frequencies is used for LW radiation towards outer space according to **figure 6**.

See **figure 4** and Pangburn blog **[2]** for further details.

The phenomenon has been confirmed to the author by le Pair **[3]**.

In the stack model we can take into account the results of Pangburn, by claiming that from the Prevost flux in **figure 3** of 46 W/m², a fraction 18 W/m² is thermalized and radiated towards outer space by the broad water vapor H₂O frequency band according to **figure 6**.

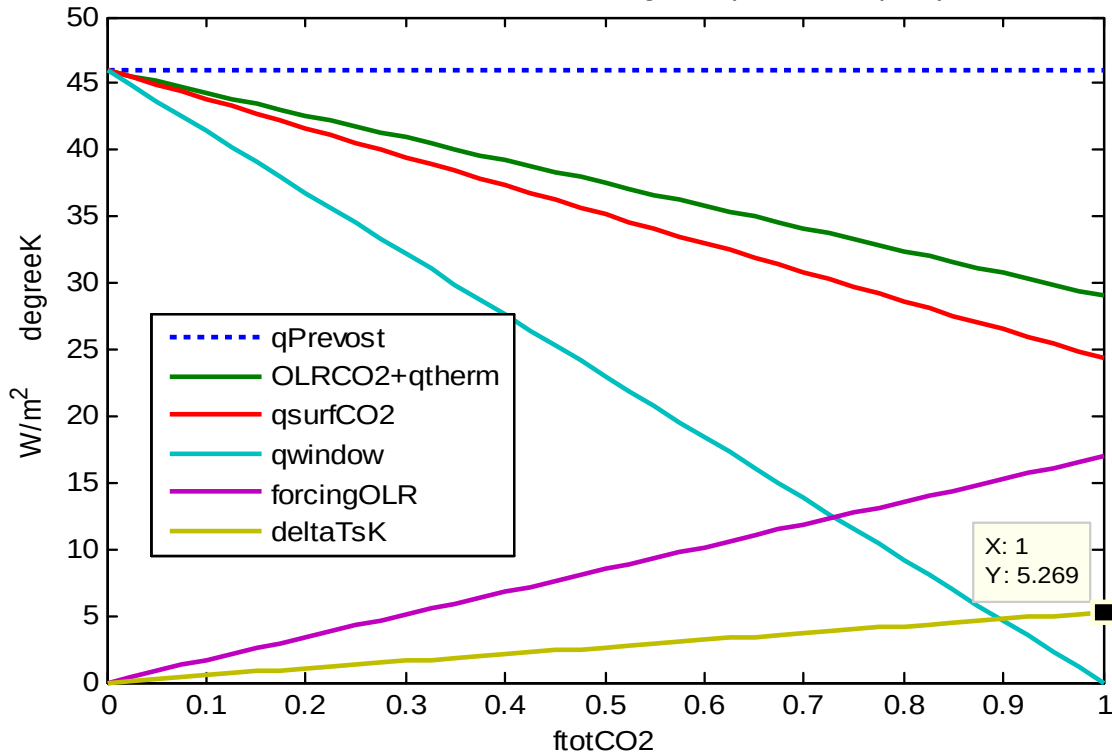
Figure 9 with a thermalization of $q_{\text{therm}} = 18 \text{ W/m}^2$ gives results for $f_{\text{totCO}_2}=0$ up to $f_{\text{totCO}_2} = 1$.

It has to be compared with **figure 8a**, which is without thermalization.

Figure 9 with thermalization, saturation not applicable for $ftotCO_2 < 1$

fig 4.1a Result of CO2

nods =90 height =30 km $ftotCO_2 = 1$ $TsK = 288.7209$ K $fractionCO_2 = 0.11675$ $qPrevost = 46$
 $dOLRdTsk = 3.2185$ $deltaTsK = forcingOLR/(dOLRdTsk)$ $qtherm = 18$



For $ftotCO_2 = 1$:

$q(1) = q_{surf} =$ surface flux LW CO2 radiation

$-q(N) = OLR =$ outgoing LW 11.04 CO2 path + 18 H2O path, total 29.04 W/m^2

Pangburn results [2] were given for $ftotCO_2 = 1$ or 400 ppm.

Between values 0 and 1 of $ftotCO_2$, it is supposed that the thermalization is linear between 0 and 18 W/m^2 .

For the pre-industrial value of $ftotCO_2 = 0.7$ or 280 ppm, we see a value $deltaTsK = 3.689$ and for $ftotCO_2 = 1$ a value $deltaTsK = 5.269$: a difference of 1.580 $^{\circ}C$.

This difference is presented in **Table1**.

In **figure 9** for $ftotCO_2 < 1$, only the thermalization is taken into account. For CO2 concentrations beyond the 400 ppm of the year AD 2015, there is not only thermalization but also saturation, as shown in **figure 10**.

Figure 10 *with both thermalization and saturation*

fig 4.1a Result of CO2

nods =90 height =30 km ftotCO2 =4 TsK =288.7209 K fractionCO2 =0.11675 qPrevost =46
dOLRdTsk = 3.2185 deltaTsK = forcingOLR/(dOLRdTsk) qtherm= 18

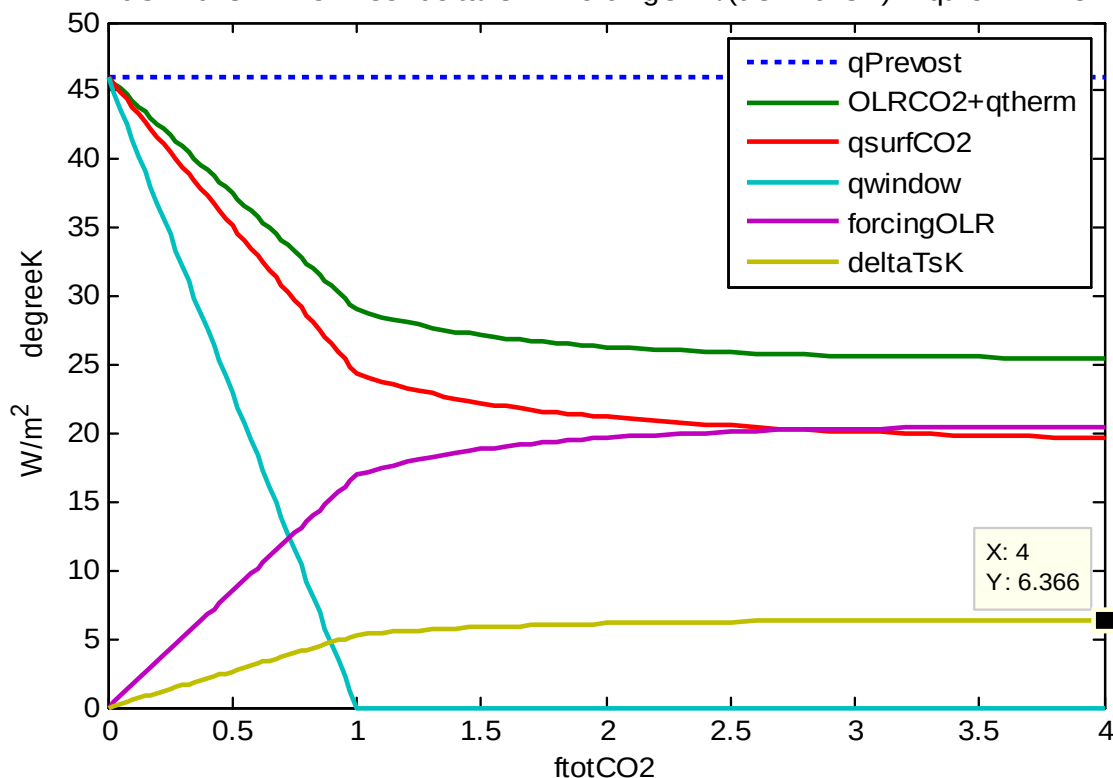


Table 1 summarizes the result of **figure 9** and **figure 10**, giving the temperature increase from $ftotCO_2 = 0$ to $ftotCO_2 = 4$, or 1600 ppm of the year AD 2615, assuming an increase of 2 ppm/yr.

Table 1

Temperature variations from $ftotCO_2 = 1$.

due to thermalization ($q_{therm} = 18 \text{ W/m}^2$) and saturation

ftotCO2	ppm	deltaTsK °C	deltaTsK -5.269 °C	year AD
0.7	280	3.689	-1.580	
1	400	5.269	0	2015
2	800	6.118	0.849	
4	1600	6.366	1.097	~ 2615

The difference of 1.580 °C between the pre-industrial 288 ppm and the AD 2015 value of 400 ppm is indeed close to the measured one of 1.5 °C.

The indicated temperature variations are only due to CO2 concentration variations and for a thermalization of 18 W/m² reported by Pangburn for CO2 concentrations of 400 ppm.

Constant sun intensity and constant cloud influences are assumed.

Conclusions

The one-stream, chicken-wire stack model for infra-red-active trace gases, already validated for the analysis of LW radiation through an atmosphere with water-vapor, has now also been applied to the analysis of CO₂ gas. The stack model deals with the issues of thermalization and saturation of CO₂ in a transparent way.

The two phenomena, thermalization and saturation of CO₂, give rise to small temperature increases, while

- before the year AD 2015 with CO₂ concentration below 400 ppm IPCC ignored thermalization, Pangburn's publication was in 2016,
- since the year AD 2016, with higher than 400 ppm CO₂, both thermalization **and** saturation of CO₂ are ignored by IPCC.

Stack results with only saturation have also been given in version II of this paper [5] with similar results for temperature increases $\Delta T_{\text{CO}_2} = 1$ to 2, as reported by Happer [4].

Thermalization of CO₂ as reported by Pangburn [2], give even lower temperature increases as compared to the saturation only analyses.

The thermalization confirms the 1.5 °C measured temperature difference of the pre-industrial period of 280 ppm CO₂ as compared to the AD 2015 period of $\Delta T_{\text{CO}_2} = 1$ or 400 ppm.

The infra-red-active gas CO₂ is harmless and non-polluting.

Until nuclear power has been installed back again, we need fossil fuels to generate electricity and for combustion engines of cars, boats and planes.

Burning fossil fuels — **fortunately** — will increase the concentration of CO₂, also called "greenhouse" gas, which indeed is used in nursery greenhouses to boost the growth of vegetables and flowers.

CO₂ is food for plants

We need more atmospheric CO₂ to feed the growing world population.

Acknowledgment

The author wants to thank Claes Johnson [6] who inspired him to write this paper based on the one-stream LW radiation to outer space, avoiding the nonphysical back-radiation. The author interpreted the one-stream proposals from Johnson by using the Stefan-Boltzmann relation all ways for a pair of surfaces, enabling the concept of standing waves between resonating infra-red-active molecules with the same eigen-frequency.

Thanks to Dan Pangburn [2] for his authorization to include **figure 4** in this paper, and his research about thermalization.

Thanks to John O'Sullivan at Principia Scientific International for the publication of this paper.

References

- [1] <https://principia-scientific.com/publications/Reynen-Finite.pdf>
- [2] Pangburn blog
https://www.researchgate.net/publication/316885439_Climate_Change_Drivers
<https://energyredirect3.blogspot.com>
- [3] Private communication 10/11/2021 from C. le Pair, The Netherlands.
- [4] Happer, <https://www.youtube.com/watch?v=PblYr-KjOVY>
(Dutch subtitles)
<https://www.youtube.com/watch?v=CA1zUW4uOSw>
(English Subtitles)
- [5] <https://principia-scientific.com/wp-content/uploads/2021/12/SaturationFinal-rev.pdf>
<https://principia-scientific.com/wp-content/uploads/2022/03/satco2paper.pdf>
<https://principia-scientific.com/wp-content/uploads/2023/02/SaturationIIIupdated.pdf>
- [6] Johnson, <https://computationalblackbody.wordpress.com/>